Inorg. Chem. **2008**, *47*, 8776−8787

Reduction of an η^2-Iminoacyl Ligand to η^2-Iminium Enabled by Adjacent Carbon Monoxide Ligand Replacement with a Variable Electron Donor Alkyne Ligand in a Cationic Tungsten(II) Bis(acetylacetonate) Complex

Andrew B. Jackson, Chetna Khosla, Peter S. White, and Joseph L. Templeton*

W.R. Kenan Laboratory, Department of Chemistry, University of North Carolina, Chapel Hill, North Carolina 27599-3290

Received April 25, 2008

Cationic iminoacyl-carbonyl tungsten complexes of the type [W(CO) (η^2-MeN═CR)(acac)$_2$]$^+$ (acac = acetylacetonate; R = Ph (**1a**), Me (**1b**)) easily undergo thermal substitution of CO with two-electron donors to yield [W(L)(η^2-MeN═CR)(acac)$_2$]$^+$ (L = *tert*-butylisonitrile [R = Ph (**2a**), Me (**2b**)], 2,6-dimethylphenylisonitrile [R = Me (**2c**)], triphenylphosphine [R = Ph (**3a**), Me (**3c**)], and tricyclohexylphosphine [R = Ph (**3b**)]). Tricyclohexylphosphine complex **3b** exhibits rapid, reversible phosphine ligand exchange at room temperature on the NMR time scale. Photolytic replacement of carbon monoxide with either phenylacetylene or 2-butyne occurs efficiently to form [W(η^2-alkyne)(η^2-MeN═CR)(acac)$_2$]$^+$ complexes (**5a-d**) with a variable electron donor η^2-alkyne paired with the η^2-iminoacyl ligand in the W(II) coordination sphere. PMe_3 adds to **1a** or **5b** to form [W(L)(η^2-MeN═C(PMe_3)Ph)(acac)$_2$]$^+$ [L = CO (**4**), MeC≡CMe (**6**)] via nucleophilic attack at the iminoacyl carbon. Addition of Na[HB(OMe)$_3$] to **5b** yields W(η^2-MeC≡CMe)(η^2-MeN═CHPh)(acac)$_2$, **8**, which exhibits alkyne rotation on the NMR time scale. Addition of MeOTf to **8** places a second methyl group on the nitrogen atom to form an unusual cationic η^2-iminium complex [W(η^2-MeC≡CMe)(η^2-Me_2N═CHPh)(acac)$_2$][OTf] (**9[OTf]**, OTf = SO_3CF_3). X-ray structures of 2,6-dimethylphenylisonitrile complex **2c[BAr′$_4$]**, tricyclohexylphosphine complex **3b[BAr′$_4$]**, and phenylacetylene complex **5a[BAr′$_4$]** confirm replacement of CO by these ligands in the [W(L)(η^2-MeN═CR)(acac)$_2$]$^+$ products. X-ray structures of alkyne-imine complexes **6[BAr′$_4$]** and **8** show products resulting from nucleophilic addition at the iminoacyl carbon, and the X-ray structure of **9[BAr′$_4$]** reflects methylation at the imine nitrogen to form a rare η^2-iminium ligand.

Introduction

Unsaturated organic molecules exhibit altered reactivity patterns once they are in the coordination sphere of a transition metal.[1−11] Specifically, nitriles readily undergo reduction when σ-bound to a metal center.[9−14] However, less is known about the reactivity of π-bound nitrile ligands.[5−8] We recently constructed a bis(acetylacetonate) tungsten(II) d^4 fragment that preferentially binds nitriles through the C≡N π-system.[15]

* To whom correspondence should be addressed. E-mail: joetemp@unc.edu.

(1) Patai, S. *Patai's Guide to the Chemistry of Functional Groups*; Wiley: Chichester, 1989.
(2) *Comprehensive Organic Functional Group Transformations*; Katritzky, A. R.; Meth-Cohn, O.; Rees, C. W., Eds.; Pergamon: Oxford, 1995; Vol. *1*−*7*.
(3) Durfee, L. D.; Rothwell, I. P. *Chem. Rev.* **1988**, *88*, 1059.
(4) Kuznetsov, M. L. *Russ. Chem. Rev.* **2002**, *71*, 265.
(5) Shin, J. H.; Savage, W.; Murphy, V. J.; Bonanno, J. B.; Churchill, D. G.; Parkin, G. *J. Chem. Soc., Dalton Trans.* **2001**, 1732.
(6) Cross, J. L.; Garrett, A. D.; Crane, T. W.; White, P. S.; Templeton, J. L. *Polyhedron* **2004**, *23*, 2831.
(7) Lis, E. C.; Delafuente, D. A.; Lin, Y.; Mocella, C. J.; Todd, M. A.; Liu, W.; Sabat, M.; Myers, W. H.; Harman, W. D. *Organometallics* **2006**, *25*, 5051.
(8) Jackson, A. B.; Khosla, C.; Gaskins, H. E.; White, P. S.; Templeton, J. L. *Organometallics* **2008**, *27*, 1322.
(9) Tsai, Y.-C.; Stephens, F. H.; Meyer, K.; Mendiratta, A.; Gheorghiu, M. D.; Cummins, C. C. *Organometallics* **2003**, *22*, 2902.
(10) Kukushkin, V. Y.; Pombeiro, A. J. L. *Chem. Rev.* **2002**, *102*, 1771.
(11) Kukushkin, V. Y.; Pombeiro, A. J. L. *Inorg. Chim. Acta* **2005**, *358*, 1.
(12) Michelin, R. A.; Mozzon, M.; Bertani, R. *Coord. Chem. Rev.* **1996**, *147*, 299.
(13) Kuznetsov, M. L.; Nazarov, A. A.; Pombeiro, A. J. L. *J. Phys. Chem. A* **2005**, *109*, 8187.
(14) Chin, C. S.; Chong, D.; Lee, B.; Jeong, H.; Won, G.; Do, Y.; Park, Y. J. *Organometallics* **2000**, *19*, 638.
(15) Jackson, A. B.; Schauer, C. K.; White, P. S.; Templeton, J. L. *J. Am. Chem. Soc.* **2007**, *129*, 10628.

10.1021/ic800738a CCC: $40.75
Published on Web 08/28/2008

Scheme 1. Facile Thermal Replacement of CO with Isonitrile

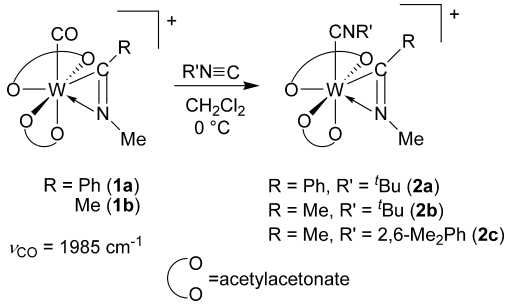

Reduction of π-bound nitrile complexes of the type W(CO)(η^2-nitrile)(acac)$_2$to neutral imine-carbonyl complexes of the general formula W(CO)(η^2-imine)(acac)$_2$ has been accomplished via stepwise addition of electrophiles and nucleophiles.[8] The η^2-imine ligand provides four electrons to tungsten in W(CO)(acac)$_2$(η^2-imine) complexes.[8,15] Attempts to convert the π-bound imine to an iminium ligand have been unproductive with carbon monoxide as the adjacent ligand in the coordination sphere. Presumably this reflects the need for a four-electron donor ligand to stabilize the six-coordinate d^4 tungsten center.[16] Addition of a second electrophile to the nitrogen of the sidebound imine ligand would remove two electrons from the metal, so electrophilic addition at nitrogen is incompatible with the simple constraints imposed by electron counting in this system.

Iminium cations[17] ($R_2N{=}CR_2^+$) are postulated as intermediates in several fundamental organic reactions including Knoevenagel condensations,[18,19] decarboxylation of β-ketoacids,[20,21] and Diels−Alder type cyclizations.[22−24] Iminium ligands in transition metal complexes have resulted from direct reactions of iminium salts with metal reagents,[25,26] from rearrangements involving group transfer to imine ligands,[27,28] from β-hydride elimination of amines,[29,30] and from nitriles using strong reductants or other harsh conditions.[31−33]

We now report conversion of an η^2-imine to an η^2-iminium ligand; this reaction is enabled by replacement of the ancillary two-electron donor CO ligand in [W(CO)(η^2-RN=CR)(acac)$_2$]$^+$ with a variable electron donor alkyne. Substitution of CO by an alkyne in the cationic iminoacyl-CO tungsten(II) reagent relieves the ligand derived from η^2-RC≡N of its responsibility to function as the sole four-electron donor to tungsten. The nitrogen lone pair of the η^2-imine ligand, datively bound to tungsten when CO is the ancillary ligand in the coordination sphere, becomes sufficiently nucleophilic to react with potent electrophiles once an alkyne replaces CO. Results presented here are complementary to reactions observed in low-valent Tp′ [Tp′ = hydridotris(3,5-dimethylpyrazolyl)borate] tungsten(II) complexes in which coordinated η^1-acetonitrile undergoes sequential reduction to an amine.[34,35]

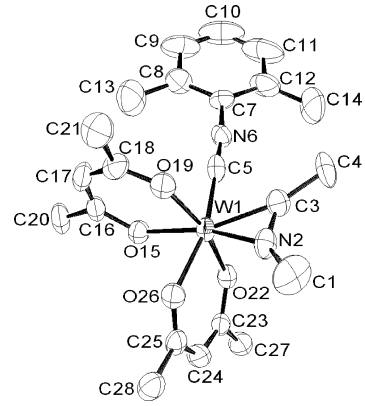

Figure 1. Oak Ridge Thermal Ellipsoid Plot (ORTEP) diagram of **2c[BAr′$_4$]**. Thermal ellipsoids are drawn with 50% probability. Hydrogen atoms, the BAr′$_4$ counterion, and 0.5 Et$_2$O are omitted for clarity.

Results and Discussion

Thermal Substitution of CO with RNC or PR$_3$ Ligands. Addition of *tert*-butylisonitrile to a cold solution of η^2-iminoacyl complex [W(CO)(η^2-MeN=CPh)(acac)$_2$]$^+$ **1a** leads to [W(CN^{t}Bu)(η^2-MeN=CPh)(acac)$_2$]$^+$ (**2a**) (Scheme 1). No CO absorbance is observed via in situ IR spectroscopy after 20 min of stirring at 0 °C; this is a surprisingly facile substitution reaction. For complex **2a**, the N-methyl resonance in the ^{1}H NMR spectrum shifts downfield to 5.67 ppm from the 4.97 ppm value of the iminoacyl-carbonyl precursor. The iminoacyl carbon resonates downfield at 239.7 ppm in the ^{13}C NMR spectrum. Low temperature ^{13}C NMR spectroscopy (240 K) reveals the metal-bound isonitrile carbon at 146.1 ppm, indicative of σ-bound isonitrile.

The solid state structure of **2c[BAr′$_4$]** (BAr′$_4$ = tetrakis[(3,5-trifluoromethyl)phenyl]borate) reflects simple substitution of the carbon monoxide ligand by 2,6-dimethylphenylisonitrile (Figure 1). The nitrogen atom of the iminoacyl ligand is *distal* with respect to the cis isonitrile ligand, thus adopting the same orientation as the parent CO complex. The W−C−N triangular geometry is barely perturbed by replacement of CO with 2,6-dimethylphenylisonitrile.

Addition of triphenylphosphine to iminoacyl cation **1a** also leads to carbon monoxide replacement. The product is an air and moisture sensitive deep purple complex, [W(PPh$_3$)(η^2-

(16) Templeton, J. L. *Adv. Organomet. Chem.* **1989**, *29*, 1.
(17) Erkkilä, A.; Majander, I.; Pihko, P. M. *Chem. Rev.* **2007**, *107*, 5416.
(18) Blanchard, K. C.; Klein, D. L.; MacDonald, J. *J. Am. Chem. Soc.* **1931**, *53*, 2809.
(19) Crowell, T. I.; Peck, D. W. *J. Am. Chem. Soc.* **1953**, *75*, 1075.
(20) Pedersen, K. J. *J. Phys. Chem.* **1934**, *38*, 559.
(21) Pedersen, K. J. *J. Am. Chem. Soc.* **1938**, *60*, 595.
(22) Baum, J. S.; Viehe, H. G. *J. Org. Chem.* **1976**, *41*, 183.
(23) Jung, M. E.; Vaccaro, W. D.; Buszek, K. R. *Tetrahedron Lett.* **1989**, *30*, 1893.
(24) Griesbeck, A. G. *J. Org. Chem.* **1989**, *54*, 4981.
(25) Sepelak, D. J.; Pierpont, C. G.; Barefield, E. K.; Budz, J. T.; Poffenberger, C. A. *J. Am. Chem. Soc.* **1976**, *98*, 6178.
(26) Wilson, R. B.; Laine, R. M. *J. Am. Chem. Soc.* **1985**, *107*, 361.
(27) Matsumoto, M.; Nakatsu, K.; Tani, K.; Nakamura, A.; Otsuka, S. *J. Am. Chem. Soc.* **1974**, *96*, 6777.
(28) Most, K.; Mösch-Zanetti, N. C.; Vidović, D.; Magull, J. *Organometallics* **2003**, *22*, 5485.
(29) Barrera, J.; Orth, S. D.; Harman, W. D. *J. Am. Chem. Soc.* **1992**, *114*, 7316.
(30) Orth, S. D.; Barrera, J.; Rowe, S. M.; Helberg, L. E.; Harman, W. D. *Inorg. Chim. Acta* **1998**, *270*, 337.
(31) Thomas, J. L. *J. Am. Chem. Soc.* **1975**, *97*, 5943.
(32) Brunner, H.; Wachter, J.; Schmidbauer, J.; Sheldrick, G. M.; Jones, P. G. *Organometallics* **1986**, *5*, 2212.
(33) Hasegawa, T.; Kwan, K. S.; Taube, H. *Inorg. Chem.* **1992**, *31*, 1598.
(34) Feng, S. G.; Templeton, J. L. *J. Am. Chem. Soc.* **1989**, *111*, 6477.
(35) Feng, S. G.; Templeton, J. L. *Organometallics* **1992**, *11*, 1295.

Scheme 2. Thermal Replacement of CO with Bulky Phosphine Reagents

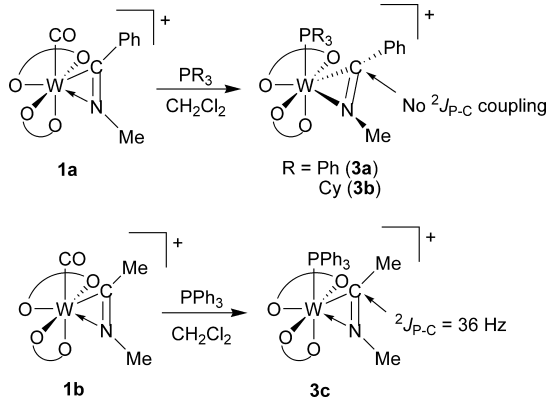

MeN═CPh)(acac)$_2$]$^+$ (**3a**) (Scheme 2). Salient spectroscopic data include a peak far downfield at 6.74 ppm in the ^{1}H NMR spectrum attributed to the nitrogen-bound methyl group; the identity of this signal was confirmed via heteronuclear multiple-bond correlation (HMBC) spectroscopy. The iminoacyl carbon resonates at 241.1 ppm in the ^{13}C NMR spectrum, and no phosphorus coupling is evident. The ^{31}P NMR spectrum displays a single resonance at −5.25 ppm with tungsten satellites [$^1J_{P-W}$ = 349 Hz, ^{183}W (14.28%), I = $^1/_2$]. These data are consistent with simple replacement of CO by PPh_3, although the intense purple color and 6.74 ppm methyl chemical shift location are surprising.

Tricyclohexylphosphine (PCy_3) also replaces the CO ligand in **1a**, and [W(PCy_3)(η^2-MeN═CPh)(acac)$_2$]$^+$ (**3b**) forms (Scheme 2). However, room temperature NMR spectroscopy shows broad resonances in ^{1}H, ^{13}C, and ^{31}P spectra. A broad peak attributed to the nitrogen-bound methyl group resonates at 8.44 ppm in the room temperature ^{1}H spectrum, a significant downfield shift from the analogous resonance in **1a**. Additionally, acetylacetonate methyl signals at 4.14 and 3.58 ppm exhibit line broadening and unusual downfield chemical shifts. The room temperature ^{13}C NMR spectrum shows broad peaks for the nitrogen-bound methyl (43.9 ppm) and two of the acetylacetonate keto-carbons (196.2 and 202.3 ppm). Room temperature ^{31}P NMR spectroscopy reveals a broad peak at −23.2 ppm devoid of tungsten satellites. Variable temperature spectra indicate a temperature dependence for the chemical shift of the nitrogen-bound methyl group. Over a temperature range of 130 degrees with CD_2Cl_2 as solvent, the methyl resonance varies from 6.94 ppm (185 K) to 8.94 ppm (315 K), broadening as the temperature increases. At 200 K, the iminoacyl carbon resonance appears at 247.1 ppm, and as in the analogous complex **3a**, shows no coupling to phosphorus. At 160 K using $CDCl_2F$ as a solvent the PCy_3 phosphorus resonance appears as a sharp singlet at 18.0 ppm ($^1J_{P-W}$ = 351 Hz).

Addition of PPh_3 to **1b** produces [W(PPh_3)(η^2-MeN═CMe)(acac)$_2$]$^+$, **3c**, over the course of several hours. This reaction with **1b** proceeds more slowly than the analogous reaction with reagent **1a**. The N-methyl group in **3c** resonates at 5.80 ppm in the ^{1}H NMR spectrum, and the

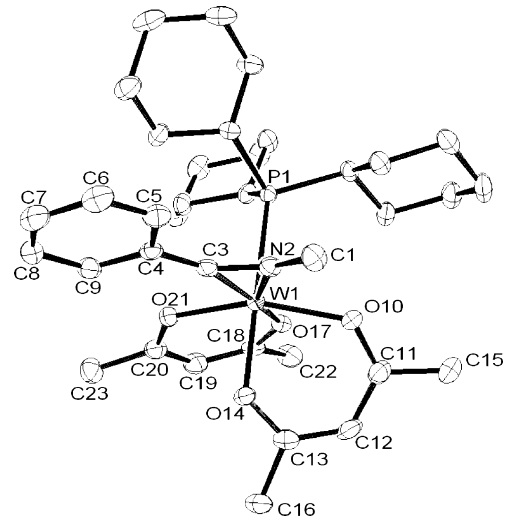

Figure 2. ORTEP diagram of **3b[BAr′$_4$]**. Thermal ellipsoids are drawn with 50% probability. Hydrogen atoms, the BAr′$_4$ counterion, and a molecule of Et_2O are omitted for clarity.

Scheme 3. Behavior of the Iminoacyl Ligand Adjacent to Bulky Phosphine Ligands

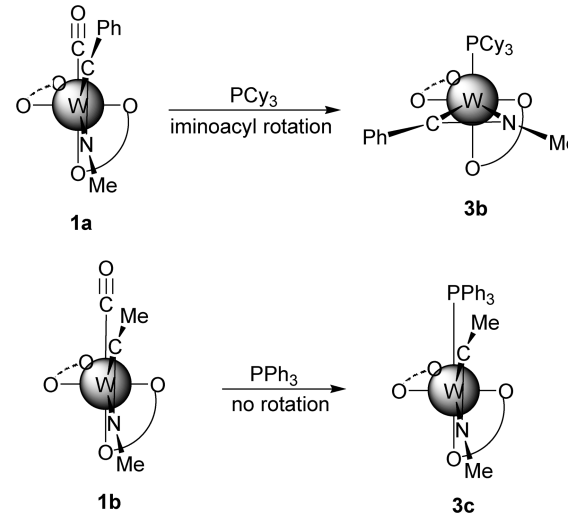

iminoacyl carbon appears as a doublet at 235.2 ppm ($^2J_{P-C}$ = 36 Hz) in the ^{13}C NMR spectrum. Note that PCy_3 does not replace CO in **1b**.

The solid state structure of [W(PCy_3)(η^2-MeN═CPh)(acac)$_2$][BAr$_4$′], **3b[BAr′$_4$]**, confirms replacement of CO with the bulky phosphine reagent (Figure 2). Most notable is a change in the W−N−C triangle orientation as the N2−C3 bond of the iminoacyl ligand is orthogonal to the new W1−P1 bond (Scheme 3). Presumably, the increased steric demand of PCy_3 in the coordination sphere forces the iminoacyl ligand to rotate 90° from the geometry observed for CO complex **1a**. The aromatic phenyl ring lies in the plane defined by the W1−N2−C3 triangle, perhaps reflecting π-delocalization. Bond distances from tungsten to the C and N atoms in the iminoacyl ligand decrease relative to the same bonds in **1a**. Considerable shortening is observed for W1−C3 (1.990(4) Å), down from 2.069(8) Å in the CO-precursor. The carbon nitrogen bond, N2−C3, lengthens 0.041 Å to 1.324(5) Å. This lengthening suggests the iminoacyl ligand receives more backbonding from tungsten after replacing the

Scheme 4. Proposed Mechanism of Reversible Tricyclohexylphosphine Dissociation

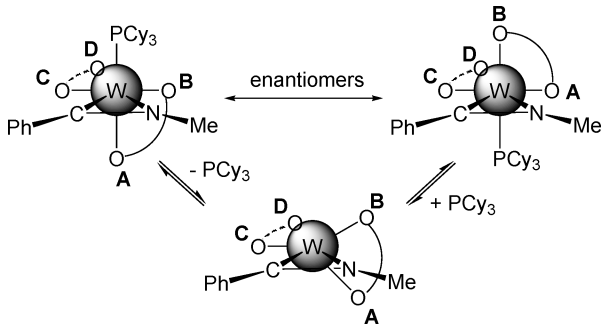

strong π-acid CO ligand with a poorer π-acid phosphine ligand. A partially solved structure of PPh_3 adduct **3c[BAr′$_4$]** clearly shows that the N=C bond remains parallel to the W−P bond suggesting that without a π-acid adjacent to the iminoacyl ligand the rotational energy profile is relatively shallow (Scheme 3). Disorder in one of the auxiliary acetylacetonate chelates prevents refinement.

Spectroscopic data indicate rapid, reversible phosphine dissociation as one process responsible for the observed fluxionality in $[W(PCy_3)(\eta^2\text{-MeN=CPh})(acac)_2]^+$. Selective line broadening is evident for this molecule with a pseudo-octahedral framework. Phosphine dissociation could allow the acetylacetonate chelate (AB) near the nitrogen-bound methyl to swing up toward the vacant coordination site, altering the geometry of the intermediate to a pseudotrigonal bipyramid with a mirror plane relating the two ends of the AB acetylacetonate that moved while leaving the other acetylacetonate (CD) in the same NMR environment (Scheme 4). Recoordination of PCy_3 could force the AB chelate either back to its original position or swing acetylacetonate AB to move end B into the position trans to PCy_3 in the octahedron, producing the enantiomer of the original complex. This mechanism explains the broad NMR resonances observed for only one acetylacetonate chelate and the phosphine, while signals for the phenyl ring and the other acetylacetonate chelate remain sharp.

The outcome of phosphine addition to **1a** reflects a dependence on the size of the phosphine reagent.[36−39] Unlike PPh_3 or PCy_3, trimethylphosphine (PMe_3) adds to **1a** at the iminoacyl carbon to form $[W(CO)(\eta^2\text{-MeN=C(PMe}_3)\text{Ph})(acac)_2]^+$ complex **4** (Scheme 5). This result mirrors reactivity observed when $Na[HB(OMe)_3]$ or MeMgBr attacks the cationic **1a** and reduces the iminoacyl ligand to an imine.[8] After PMe_3 addition, IR spectroscopy shows a single CO absorbance at 1904 cm^{-1}, a decrease of ∼80 cm^{-1} from ν_{CO} in the starting material. Addition of PMe_3 to the iminoacyl carbon indirectly pushes electron density to the metal center. ^{1}H NMR spectroscopy shows two diastereomers in an approximate ratio of 2:1. ^{13}C NMR spectroscopy supports

Scheme 5. Nucleophilic Attack at the Iminoacyl Carbon with PMe_3

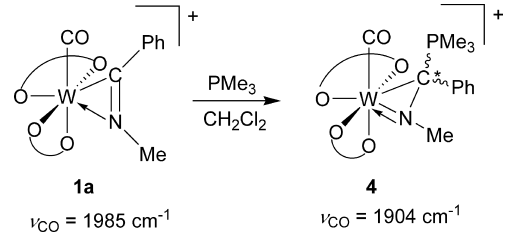

Scheme 6. Photolytic Replacement of CO with Alkyne Reagents

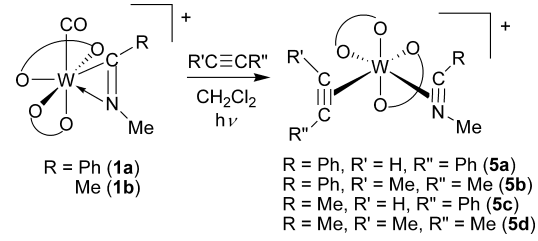

the imine-like nature of the sidebound ligand: a doublet assigned to the "imine" carbon for the major diastereomer resonates at 50.9 ppm ($^1J_{P-C}$ = 84 Hz). A doublet centered at 241.1 ppm with phosphorus coupling ($^3J_{P-C}$ = 8 Hz) is assigned to the CO carbon. Similar results were obtained using PMe_2Ph as a reagent, so the PMe_3 and PMe_2Ph products reflect attack at the iminoacyl carbon, while the larger PPh_3 and PCy_3 ligands replace CO in the coordination sphere of tungsten.

Photolytic Replacement of CO with Alkyne. Because of the propensity of tungsten(II) to bind a four-electron donor ligand in a six-coordinate environment,[8,15,40] we investigated replacement of CO with alkyne ligands. Unlike linearly ligating π-acid carbon monoxide ligands, alkynes are excellent single-faced π-acids, and additionally alkynes can serve as variable electrons donor ligands through their $\pi_\perp$ electrons.[16] This π-donor feature has the ability to alter the behavior of the adjacent η^2-iminoacyl ligand.

Refluxing phenylacetylene and **1a** in THF produces a small amount of $[W(\eta^2\text{-PhC≡CH})(\eta^2\text{-MeN=CPh})(acac)_2]^+$, **5a**. On the other hand, photolysis in methylene chloride produces the alkyne-iminoacyl cation in good yields (65−75%) (Scheme 6).

Note that for an unsymmetrical alkyne, four NMR distinguishable isomers are possible (Figure 3). Each of the four isomers shown has an enantiomer to total eight isomers. All four alkyne-iminoacyl derivatives, including the two phenylacetylene and the two 2-butyne complexes, yield two isomers as observed by NMR spectroscopy. The isomer distribution is independent of the symmetry of the alkyne and is compatible with a single alkyne orientation relative to the two acetylacetonate chelates combined with two iminoacyl orientations. The room temperature ^{1}H NMR spectrum of the phenylacetylene adduct, **5a**, shows two isomers in a 3:1 ratio. The terminal alkyne proton on the phenylacetylene ligand for the major isomer resonates downfield at 13.45 ppm in the region typical of four-electron

(36) Pearson, J.; Cooke, J.; Takats, J.; Jordan, R. B. *J. Am. Chem. Soc.* **1998**, *120*, 1434.
(37) Hamilton, D. H.; Shapley, J. R. *Organometallics* **2000**, *19*, 761.
(38) Reid, S. M.; Mague, J. T.; Fink, M. J. *J. Am. Chem. Soc.* **2001**, *123*, 4081.
(39) Dennett, J. N. L.; Ferguson, M. J.; McDonald, R.; Takats, J. *Can. J. Chem.* **2005**, *83*, 862.
(40) Jackson, A. B.; White, P. S.; Templeton, J. L. *Inorg. Chem.* **2006**, *45*, 6205.

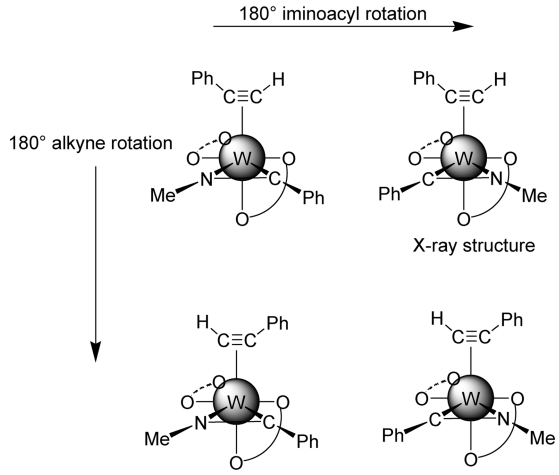

Figure 3. Four possible isomers of asymmetric alkyne derivative **5a**.

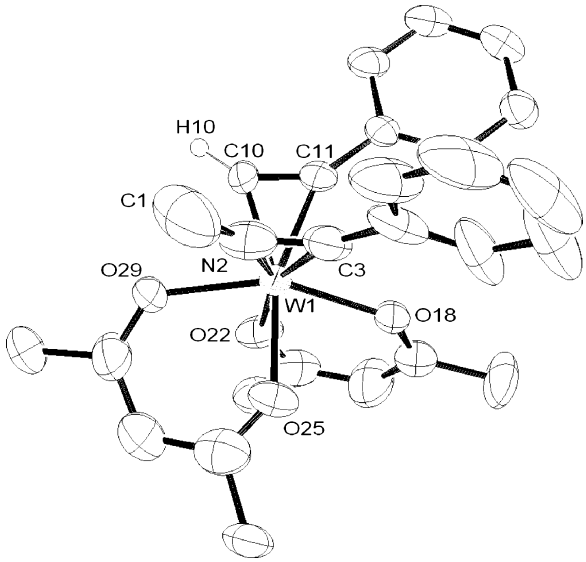

Figure 4. ORTEP diagram of **5a[BAr′4]**. Thermal ellipsoids are drawn with 50% probability. Non-essential hydrogen atoms and the BAr'_4 counterion are omitted for clarity.

donor alkynes. Both the alkyne and the iminoacyl ligands appear to be static on the NMR time scale. At room temperature the ^{13}C NMR spectrum of **5a** shows the iminoacyl carbon resonance at 217.0 ppm. The alkyne carbons of the major isomer resonate at 208.2 (Ph*C*≡CH) and 204.6 ppm (PhC≡*C*H).

The solid state structure of the cationic alkyne-iminoacyl complex **5a[BAr′4]** shows the iminoacyl ligand is rotated 90° relative to reagent **1a[OTf]**. The C−N linkage in **5a[BAr′4]** is roughly parallel to the trans O−W−O axis (Figure 4). The alkyne and iminoacyl ligands are (i) π-bound to the metal, (ii) *cis* to each other, and (iii) parallel to one another. The N-methyl group is *proximal* to the terminal alkyne proton on the phenylacetylene ligand, and the two phenyl rings are *proximal* to each other. In spite of the π-donor capability of the alkyne ligand, the two bonds from tungsten to the iminoacyl differ only slightly from those in the precursor carbonyl-iminoacyl cation. The W1−C3 bond is 2.052(9) Å, and the W1−N2 bond is 1.990(8) Å.

Displacement of Triphenylphosphine. The triphenylphosphine ligand in **3a** can be easily displaced by either isonitrile

Scheme 7. Displacement of Triphenylphosphine with Either Isonitrile or Alkyne Reagents

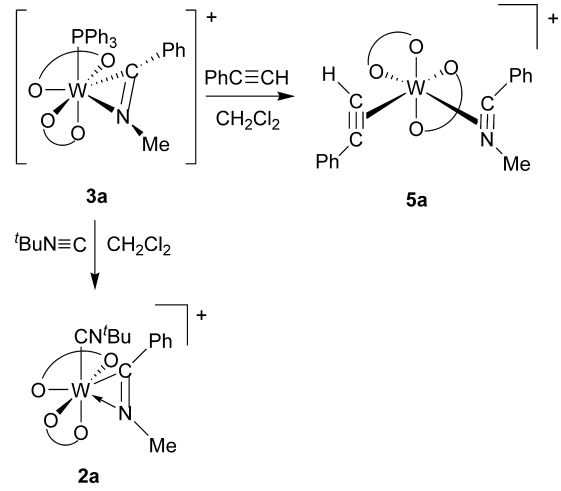

or alkyne reagents (Scheme 7). Following generation of **3a** in situ, addition of *tert*-butylisonitrile or phenylacetylene quickly forms either **2a** or **5a**, respectively, as confirmed by ^1H NMR spectroscopy. This stepwise substitution methodology provides an attractive, two-step thermal route to complexes **5a**−**d** as an alternative to photolytic preparation.

Orbital Interactions and Electron Counting. Cationic iminoacyl bis(acac) complexes **1a** and **1b** can be mapped to the same MO model as analogous neutral bis(acac) η^2-alkyne or η^2-nitrile complexes in terms of electron donation from the iminoacyl ligand and the oxidation state of the tungsten center (Figure 5). If the neutral $W(L)(acac)_2$ (L = CO, CNR) fragment is counted as a low valent W(II) d^4 fourteen-electron moiety, four electrons must be supplied from the cationic iminoacyl ligand ($MeN{=}C^+R$), equivalent to a nitrilium ($MeN^+{\equiv}CR$), to optimally utilize the available electrons and orbitals. Carbon monoxide or isonitrile, situated along the *z*-axis, will stabilize the dπ orbitals with *z*-character, and thus dictate the location of the four W(II) metal-based electrons. Binding the cationic iminoacyl fragment along the *x*-axis further stabilizes d_{xz} via backbonding, and also pushes the empty d_{xy} orbital up in energy as the antibonding component reflecting donation from the filled $\pi_\perp$ orbital on the $MeN^+{\equiv}CR$ ligand. This bonding description treats the cationic four-electron donor ligand like an alkyne. The

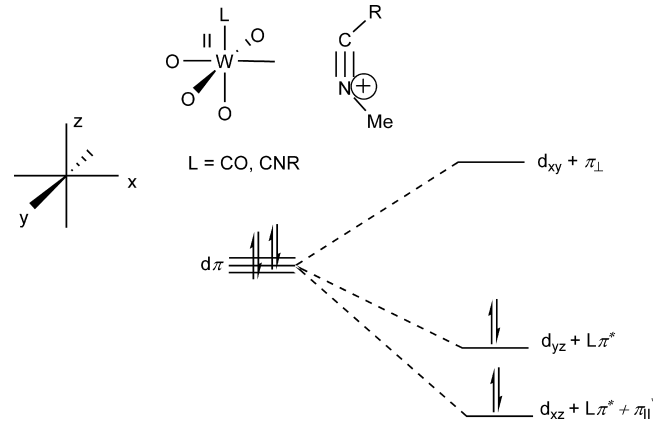

Figure 5. Orbital diagram for **1** and **2**.

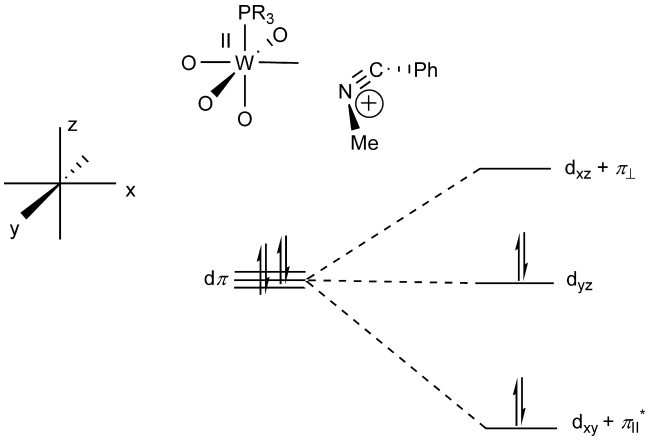

Figure 6. Orbital diagram for **3a** and **3b**.

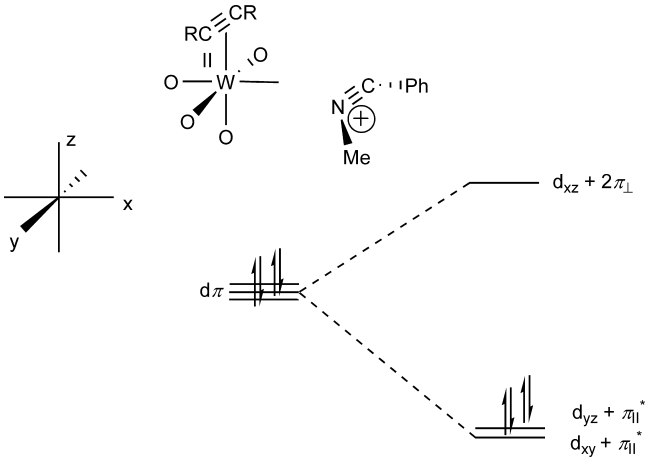

Figure 7. Orbital diagram for **5**.

transparency of mapping $RN^+{\equiv}CR$ onto $RC{\equiv}CR$ leads us to favor this description for building a simple MO picture, but it is worthwhile to note that the final result can be constructed using $RN{=}C^-{-}R$ and a d^2 W(IV) formalism with the anionic η^2-iminoacyl providing a total of six electrons to the metal.

A different orbital diagram emerges for phosphine complex **3a** (Figure 6). No significant stabilization of the four $d\pi$ electrons is expected from the phosphine. With no dominant electronic preference for binding the η^2-NC ligand either parallel or orthogonal to the W−P bond, the steric interactions between the bulky phosphine ligand and the phenyl ring favor the observed orthogonal orientation of the iminoacyl ligand. The intense color and rapid decomposition upon exposure to air are compatible with a high lying highest occupied molecular orbital (HOMO) that lacks stabilization by a π-acid ligand.

In contrast, complexes **5a**−**d** feature a variable electron donor alkyne that also serves as a single faced π-acid capable of stabilizing the filled d_{yz} orbital while the iminoacyl ligand stabilizes the filled d_{xy} orbital (Figure 7). Both of these π-bound ligands compete to donate electrons from their respective $\pi_\perp$ orbitals into the empty d_{xz} orbital, and the result is a three-center four-electron interaction. This outcome tracks orbital diagrams describing M(II)bis(alkyne) (M = Mo, W) complexes,[41,42] but the symmetry of two equivalent alkyne donors is broken.[43] Spectroscopic and structural data imply that the alkyne ligand contributes more electron density into d_{xz} than the iminoacyl ligand in accord with electronegativity expectations. In the end a total of six electrons will be donated from the two η^2-ligands, but combinations along a continuum ranging from 2+4 through 3+3 to 4+2 from the iminoacyl and alkyne ligands, respectively, are conceivable in the absence of symmetry constraints.

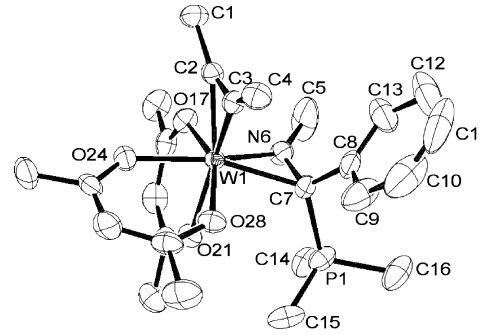

Figure 8. ORTEP diagram of **6[BAr′4]**. Thermal ellipsoids are drawn with 50% probability. Hydrogen atoms and the BAr'_4 counterion are omitted for clarity.

Scheme 8. Nucleophilic Attack by PMe_3 at Iminoacyl Carbon in **5b**

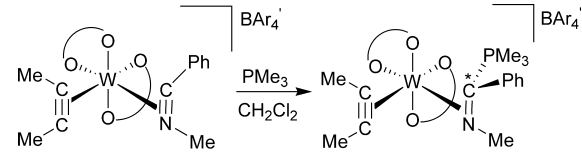

Phosphine Addition to Cationic Iminoacyl-Alkyne Complexes. Addition of PMe_3 to **5b[BAr′4]** produces the cationic imine complex $[W(\eta^2\text{-MeC}{\equiv}\text{CMe})(\eta^2\text{-MeN}{=}\text{C}(PMe_3)\text{Ph})(\text{acac})_2][BAr'_4]$, **6[BAr′4]**, (Scheme 8). Two isomers are present in a ratio of ∼20:1. Room temperature ^{1}H NMR data reveal hindered rotation of the alkyne as evidenced by a broad singlet for each methyl group on 2-butyne (2.78 and 1.42 ppm). Additionally, the *ortho* and *meta* phenyl protons are broad indicating hindered rotation of the phenyl ring. Low temperature NMR studies show sharpening and shifting of alkyne and phenyl resonances, eventually slowing rotation of the phenyl ring to reveal five distinct resonances at 203 K. ^{13}C NMR data indicate decreased electron donation from the alkyne in **6** with resonances at 182.7 and 182.8 ppm compared to the alkyne in **5b** which has ^{13}C signals at 208 ppm. The former iminoacyl carbon shifts upfield to 52.8 ppm in **6** from 217.5 ppm in **5b**. In spite of the direct P−C connection, no phosphorus coupling can be distinguished in this broad C-13 resonance. The solid state structure shows retention of the basic connectivity of **5a** (Figure 8). The high diastereoselectivity (20:1) contrasts with the poor stereoselectivity

(41) Herrick, R. S.; Templeton, J. L. *Organometallics* **1982**, *1*, 842.
(42) Herrick, R. S.; Burgmayer, S. J. N.; Templeton, J. L. *Inorg. Chem.* **1983**, *22*, 3275.
(43) Etienne, M.; Carfagna, C.; Lorente, P.; Mathieu, R.; de Montauzon, D. *Organometallics* **1999**, *18*, 3075.

Scheme 9. Nucleophilic Attack of **5a** by PMe_3 at the Terminal Carbon of η^2-PhC≡CH

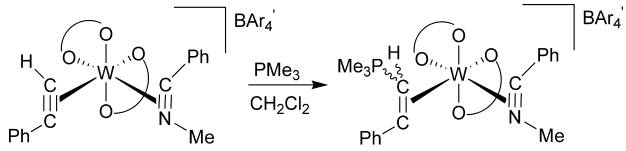

5a **7**

Scheme 10. Addition of Na[HB(OMe)$_3$] to Produce the Alkyne-Imine Complex **8**

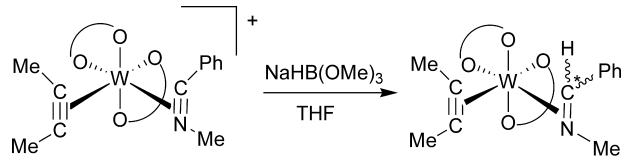

5b **8**

observed in the analogous reaction to form complex **4** from the CO complex **1a** (d.r. ~ 2:1) discussed above.

With a terminal alkyne adjacent to the iminoacyl ligand in **5a[BAr′$_4$]**, addition of PMe_3 generates an η^2-vinyl species, [W(η^2-MeN=CPh)(η^2-PhC=C(H)PMe$_3$)(acac)$_2$][BAr′$_4$], **7-[BAr′$_4$]**, via attack at the terminal alkyne carbon of the coordinated phenylacetylene (Scheme 9). ^{1}H NMR spectroscopy confirms the presence of four isomers in a 10:4:3:2 ratio, and no acetylene proton is present at low field. The former acetylenic proton resonates at 3.04 ppm ($^2J_{P-H}$ = 27 Hz) in the major isomer. The ^{13}C NMR spectrum shows a resonance at 31.6 ppm ($^1J_{P-C}$ = 85 Hz) corresponding to the four-coordinate η^2-vinyl carbon as confirmed with HMQC spectroscopy. The other vinyl carbon resonates at 241 ppm, indicating alkylidene character. These resonances are typical of η^2-vinyl ligands, also known as metallocyclopropenes. Examples of η^2-vinyls generated by nucleophilic attack on a terminal η^2-alkyne ligand have been known for some time.[45,46]

Reduction of the Iminoacyl Ligand. Addition of Na[HB(OMe)$_3$] to [W(η^2-MeC≡CMe)(η^2-MeN=CPh)(acac)$_2$]$^+$, **5b**, in tetrahydrofuran (THF) results in hydride addition to form W(η^2-MeC≡CMe) (η^2-MeN=CHPh)(acac)$_2$, **8**, (Scheme 10). The molecule is fluxional at room temperature in solution, and NMR peak assignments were based on low temperature spectra. At 200 K, rearrangement processes are sufficiently slow to reveal the presence of four isomers (two diastereomers for both imine orientations) resulting from hydride addition at the iminoacyl carbon. The hydride added to form the imine resonates at 2.40 ppm in the major isomer of **8**, well upfield from the analogous resonance of the comparable carbonyl-imine complex at 5.56 ppm.[8]

One fluxional process in **8** that has no bearing on the isomer distribution is rotation of the 2-butyne ligand. Coalescence for 2-butyne rotation occurs at 247 K, corresponding to a free energy value of 14.3 kcal/mol.[44] At 200 K the imine carbon in the major isomer resonates at 73.6 ppm in the ^{13}C NMR spectrum reflecting hybridization to a pseudotetrahedral sp^3 carbon resulting from hydride addition. The two alkyne carbons in the major isomer resonate at 204.7 and 208.7 ppm.

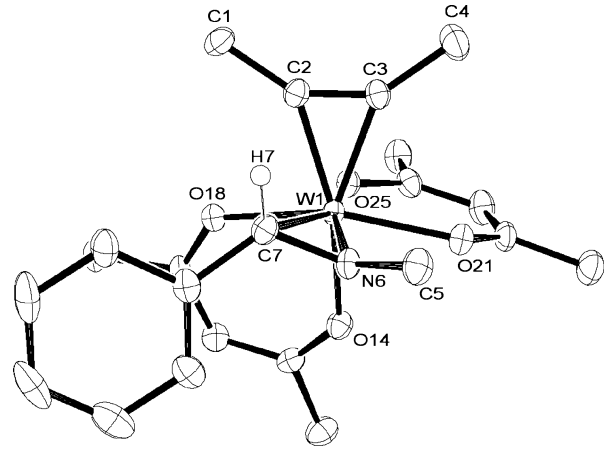

Figure 9. ORTEP diagram of **8**. Thermal ellipsoids are drawn with 50% probability. Non-essential hydrogen atoms are omitted for clarity.

Scheme 11. Alkylation with MeOTf to Form the Alkyne-Iminium Complex **9[OTf]**

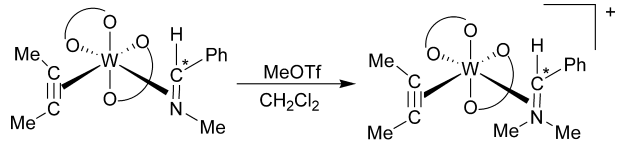

8 **9**

X-ray data for **8** reveal the phenyl ring of the iminoacyl ligand lying over the adjacent acetylacetonate chelate. This contrasts with structures for **3b** and **5a** in which the N-methyl group lies near the chelate ring in the two cis positions. Significant lengthening of both the tungsten−carbon bond [W1−C7 = 2.220(3) Å, (+0.168 Å)] and the nitrogen−carbon bond [N6−C7 = 1.395(4) Å, (+0.134 Å)] results from hydride addition to form the imine, consistent with reduction to form an sp^3 hybridized carbon. (Figure 9).

Formation of a Coordinated Iminium. Alkylation of complex **8** with MeOTf yields four isomers of [W(η^2-MeC≡CMe)(η^2-Me$_2$N=CHPh)(acac)$_2$][OTf], **9[OTf]** (Scheme 11). The proton attached to the iminium carbon resonates at 3.99 ppm (major), a downfield shift from the value observed for **8** (2.40 ppm). The diastereotopic nitrogen-bound methyl groups appear as singlets at 2.97 and 2.68 ppm, and the terminal methyl groups on the 2-butyne ligand coincide at 2.82 ppm, probably because of rapid alkyne rotation. The ^{13}C NMR spectrum clearly supports the role of the alkyne ligand as the lone four-electron donor in **7**; the two alkyne carbons resonate at 240 ppm. This chemical shift reflects the role of the η^2-iminium fragment as a simple two-electron donor. The iminium carbon appears at 91 ppm. Overall, the original benzonitrile ligand[15] undergoes three additions (electrophile, nucleophile, electrophile) and is formally reduced to a coordinated iminium fragment.

(44) Gutowsky, H. S.; Holm, C. H. *J. Chem. Phys.* **1956**, *25*, 1228.
(45) Morrow, J. R.; Tonker, T. L.; Templeton, J. L. *J. Am. Chem. Soc.* **1985**, *107*, 6956.
(46) Frohnapfel, D. S.; Templeton, J. L. *Coord. Chem. Rev.* **2000**, *206*, 199.

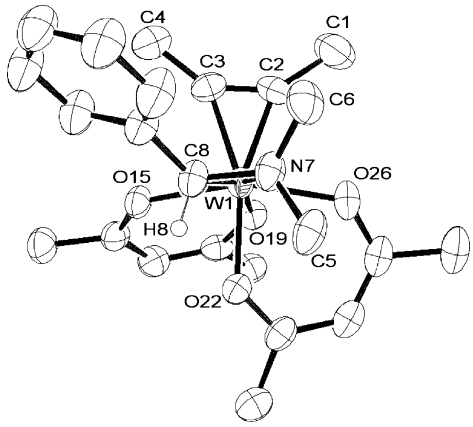

Figure 10. ORTEP diagram of **9[BAr′$_4$]**. Thermal ellipsoids are drawn with 50% probability. Non-essential hydrogen atoms and the BAr′$_4$ counterion are omitted for clarity.

The solid state structure shows the added methyl group is bound to the η^2-iminium nitrogen and both N7 and C8 of the iminium ligand assume a tetrahedral geometry (Figure 10). The W1−N7 linkage lengthens substantially to 2.190(4) Å, reflecting a loss of double bond character present in the neutral precursor molecule (1.952(3) Å).

Summary

The carbon monoxide ligand in the cationic iminoacyl-carbonyl complexes (**1a** or **1b**) is easily displaced thermally with either isonitrile or bulky phosphine reagents, or photolytically with alkyne reagents to form [W(L)(η^2-MeN═CR)(acac)$_2$]$^+$ [L = ^{t}BuNC, 2,6-Me$_2$PhNC, PPh$_3$, PCy$_3$, PhC≡CH, MeC≡CMe] complexes. Trimethylphosphine attacks the iminoacyl carbon in these cationic complexes to form [W(L)(η^2-MeN-C(PMe$_3$)Ph)(acac)$_2$]$^+$ (L = CO, 2-butyne) complexes. Replacement of the π-acid CO ligand with a four-electron donor alkyne allows further reduction of the iminoacyl ligand to a sidebound iminium ligand via hydride addition and subsequent methylation.

Experimental Section

General Information. All air-and moisture-sensitive materials were handled using Schlenk or glovebox techniques under a dry nitrogen or argon atmosphere, respectively. All glassware was oven-dried before use. Methylene chloride, diethyl ether, hexanes, and pentane were purified by passage through an activated alumina column under a dry argon atmosphere.[47] THF was distilled from a sodium ketal suspension. Methylene chloride-d_2 was dried over CaH_2 and degassed. Complexes **1a[OTf]** and **1b[OTf]**[8] and NaBAr′$_4$[48] were made in accordance with literature procedures. All other reagents were purchased from commercial sources and used without further purification. NMR data are given for one salt (OTf or BAr′$_4$); chemical shift differences between the two salts are negligible.

NMR spectra were recorded on Bruker DRX400, AMX400, or AMX300 spectrometers. Phosphorus chemical shifts were referenced to H_3PO_4 as an external standard. Infrared spectra were recorded on an ASI Applied Systems React IR 1000 FT-IR spectrometer. Elemental analysis was preformed by Atlantic Mircrolab, Norcross, GA, and Robertson Microlit, Madison, NJ. Mass spectra (MS) and high resolution mass spectra (HRMS) were acquired with a Bruker BioTOF II reflectron time-of-flight (reTOF) mass spectrometer equipped with an Apollo electrospray ionization (ESI) source. Mass spectral data are reported for the most abundant tungsten isotope. Crystal and data collection parameters as well as salient crystallographic and spectroscopic data are presented in Tables 1−3.

Representative [BAr′$_4$]$^-$ NMR Data. ^{1}H and ^{13}C NMR data for the [BAr′$_4$]$^-$ counterion are reported separately for simplicity. ^{1}H NMR (CD_2Cl_2, 193 K, δ): 7.77 (br, 8H, *o*-Ar′), 7.60 (br, 4H, *p*-Ar′). ^{13}C{^{1}H} NMR (CD_2Cl_2, 193 K, δ): 162.2 (1:1:1:1 pattern, $^1J_{B-C}$ = 50 Hz, C_{ipso}), 135.3 (C_{ortho}), 129.4 (qq, $^2J_{C-F}$ = 30 Hz, $^4J_{C-F}$ = 5 Hz, C_{meta}), 125.1 (q, $^1J_{C-F}$ = 270 Hz, CF_3), 117.9 (C_{para}).

[W(CO)(η^2-MeN═CPh)(acac)$_2$][BAr′$_4$] (1a[BAr′$_4$]). 1a[OTf] (0.305 g, 0.450mmol) was dissolved in methylene chloride, and NaBAr′$_4$ (0.398 g, 0.449 mmol) was added under a backflow of N_2. The solution was stirred for 2 h and cannula filtered away from the residual sodium salts. The red-brown solid was triturated with methylene chloride and hexanes to yield a brown powder (0.450 g, 0.323 mmol, 72%).

[W(CO)(η^2-MeN═CMe)(acac)$_2$][BAr′$_4$] (1b[BAr′$_4$]). 1b[OTf] (0.22 g, 0.36 mmol) was dissolved in methylene chloride, and NaBAr′$_4$ (0.35 g, 0.39 mmol) was added under a backflow of N_2. The solution was stirred for 1 h and cannula filtered away from the residual sodium salts. The green-brown solid was triturated with methylene chloride and hexanes to yield a green-brown powder (0.350 g, 0.27 mmol, 76%).

[W(CN^{t}Bu)(η^2-MeN═CPh)(acac)$_2$][OTf] (2a[OTf]). A 100 mL Schlenk flask was charged with **1a[OTf]** (85 mg, 0.13 mmol) which was dissolved in methylene chloride (10 mL) at 0 °C resulting in a burgundy solution. Addition of *tert*-butylisonitrile (20 μL, 0.17 mmol) caused a color change from burgundy to deep purple within 5 min. IR spectroscopy indicated no metal−carbonyl absorbances. Hexanes were added to precipitate a dark purple powder (35 mg, 0.048 mmol, 38%). ^{1}H NMR (CD_2Cl_2, 298 K, δ): 7.77−7.81 (m, 2H, *m*-C_6H_5), 7.62−7.65 (m, 2H, *o*-C_6H_5), 7.38−7.42 (m, 1H, *p*-C_6H_5), 5.81, 5.90 (each a s, each 1H, acac C*H*), 5.67 (s, 3H, N−CH_3), 2.88, 2.59, 2.34, 2.15 (each a s, each 3H, acac CH_3), 1.46 (s, 9H, -(CH_3)$_3$). ^{13}C{^{1}H} NMR (CD_2Cl_2, 298 K, δ): 25.0, 25.1, 26.4, 28.0 (acac *C*H$_3$), 32.0 (-(*C*H$_3$)$_3$), 40.0 (N−*C*H$_3$), 59.4 (CN−*C*−(CH$_3$)$_3$), 98.7, 102.9 (acac *C*H), 128.0 (*p*-C_6H_5), 128.6, 133.3 (*o/m*-C_6H_5), 135.7 (*ipso*-C_6H_5), 146.5 (*C*N^{t}Bu), 189.5, 190.0, 191.6, 200.0 (acac *C*O), 234.4 (N═*C*). MS (ESI) *m*/*z* Calc.: 583.2 (M$^+$), 500.1 (M$^+$ − ^{t}BuNC). Found: 583.2, 500.1.

[W(CN^{t}Bu)(η^2-MeN═CMe)(acac)$_2$][BAr′$_4$] (2b[BAr′$_4$]). 1b[BAr′$_4$] (51 mg, 0.038 mmol) was dissolved in methylene chloride (10 mL) in a 100 mL Schlenk flask resulting in an olive green solution. Addition of *tert*-butylisonitrile (10 μL, 0.084 mmol) at 0 °C caused a color change to red over 30 min of stirring. Hexanes (25 mL) were added to precipitate a red solid (45 mg, 0.033 mmol, 85%). ^{1}H NMR (CD_2Cl_2, 298 K, δ): 5.82, 5.73 (each a s, each 1H, acac C*H*), 5.38 (s, 3H, N−CH_3), 4.63 (s, 3H, N═C−CH_3), 2.86, 2.55, 2.25, 2.10 (each a s, each 3H, acac CH_3), 1.50 (s, 9H, C−(CH_3)$_3$). ^{13}C{^{1}H} NMR (CD_2Cl_2, 298 K, δ): 18.6 (N═C−*C*H$_3$), 24.7, 24.9, 26.3, 27.8 (acac *C*H$_3$), 32.8 (C−(*C*H$_3$)$_3$), 38.3 (N−*C*H$_3$), 59.4 (*C*−(CH$_3$)$_3$), 98.7, 102.3 (acac *C*H), 189.7, 190.2, 191.9, 200.3 (acac *C*O), 240.2 (N═*C*). ^{13}C{^{1}H} NMR (CD_2Cl_2, 240 K, δ): 146.2 (*C*N^{t}Bu). HRMS (ESI) *m*/*z* Calc.: 521.163 (M$^+$), 438.089 (M$^+$ − ^{t}BuNC). Found: 521.148, 438.071.

[W(2,6-dimethylphenylisonitrile)(η^2-MeN═CMe)(acac)$_2$][BAr′$_4$] (2c[BAr′$_4$]). A 100 mL Schlenk flask was charged with **1b[BAr′$_4$]** (55 mg, 0.041 mmol) which was dissolved in methylene chloride

(47) Pangborn, A. B.; Giardello, M. A.; Grubbs, R. H.; Rosen, R. K.; Timmers, F. J. *Organometallics* **1996**, *15*, 1518.
(48) Yakelis, N. A.; Bergman, R. G. *Organometallics* **2005**, *24*, 3579.

Table 1. Crystal and Data Collection Parameters for [W(CN-$C_6H_3Me_2$)(η^2-MeN=CMe)(acac)$_2$][BAr′$_4$] (**2c[BAr′$_4$]**); [W(PCy_3)(η^2-MeN=CPh)(acac)$_2$][BAr′$_4$] (**3b[BAr′$_4$]**); and [W(η^2-PhC≡CH)(η^2-MeN=CPh)(acac)$_2$][BAr′$_4$] (**5a[BAr′$_4$]**)

complex	**2c[BAr′$_4$]**	**3b[BAr′$_4$]**	**5a[BAr′$_4$]**
empirical formula	$C_{54}H_{41}BF_{24}N_2O_4W$ $^1/_2Et_2O$	$C_{68}H_{67}BF_{24}NO_4PW \cdot Et_2O$	$C_{58}H_{40}BF_{24}NO_4W$
fw	1469.61	1717.98	1465.57
color	red/brown	purple	yellow
T (K)	100(2)	100(2)	100(2)
λ (Å)	0.71703	0.71703	0.71703
cryst syst	triclinic	triclinic	triclinic
space group	$P\bar{1}$	$P\bar{1}$	$P\bar{1}$
a (Å)	13.0368(4)	12.5105(2)	12.9884(4)
b (Å)	13.0932(3)	16.0383(3)	14.3778(5)
c (Å)	20.0413(6)	19.8966(4)	17.9290(6)
α (deg)	76.898(2)	70.525(1)	111.900(2)
β (deg)	80.350(2)	86.315(1)	99.667(2)
γ (deg)	78.311(2)	84.339(1)	99.845(2)
vol. (Å^3)	3236.10(16)	3740.65(12)	2960.84(17)
Z	2	2	2
ρ_{calcd} (mg/m^3)	1.508	1.525	1.644
μ, mm^{-1}	1.90	1.674	2.073
F(000)	1454	1732	1444
crystal size (mm^3)	0.20 × 0.20 × 0.05	0.25 × 0.20 × 0.15	0.15 × 0.15 × 0.10
2θ range (deg)	1.05 to 25.00	1.09 to 26.51	1.64 to 25.00
index ranges	$-15 \le h \le 15$	$-15 \le h \le 15$	$-15 \le h \le 15$
	$-11 \le k \le 14$	$-20 \le k \le 20$	$-17 \le k \le 17$
	$-23 \le l \le 19$	$-22 \le l \le 24$	$-21 \le l \le 21$
reflections collected	24028	51721	43710
independent reflections	11344	15443	10391
data/restraints/parameters	11344/0/798	15443/138/1007	10391/0/808
goodness-of-fit on F^2	1.018	1.024	1.074
R1, wR2[$I > 2\sigma(I)$]	0.0663, 0.1725	0.0357, 0.0822	0.0611, 0.1361
R1, wR2 (all data)	0.1088, 0.2064	0.0458, 0.0878	0.0789, 0.1450

Table 2. Crystal and Data Collection Parameters for [W(η^2-MeC≡CMe)(η^2-MeN=C(PMe_3)Ph) (acac)$_2$][BAr′$_4$] (**6[BAr′$_4$]**); W(η^2-MeC≡CMe)(η^2-MeN=CHPh)(acac)$_2$ (**8**); and [W(η^2-MeC≡CMe)(η^2-Me_2N=CHPh)(acac)$_2$][BAr′$_4$] (**9[BAr′$_4$]**)

complex	**6[BAr′$_4$]**	**8**	**9[BAr′$_4$]**
empirical formula	$C_{57}H_{49}BF_{24}NO_4PW$	$C_{22}H_{29}NO_4W$	$C_{55}H_{44}BF_{24}NO_4W$
fw	1493.60	555.31	1433.57
color	yellow	orange	orange
T (K)	100(2) K	100(2) K	100(2) K
λ (Å)	0.71073	0.71703 Å	1.54178
cryst syst	monoclinic	triclinic	triclinic
space group	$P2_{1/c}$	$P\bar{1}$	$P\bar{1}$
a (Å)	12.7556(3)	8.4166(11)	12.4372(3)
b (Å)	19.0951(5)	10.2419(13)	12.7720(3)
c (Å)	24.7718(6)	13.3165(19)	18.6366(5)
α (deg)	90	99.903(6)	87.162(1)
β (deg)	96.020(1)	97.032(7)	80.333(1)
γ (deg)	90	92.263(6)	79.078(1)
vol. (Å^3)	6000.4(3)	1120.1(3)	2865.01(12)
Z	4	2	2
ρ_{calcd} (mg/m^3)	1.653	1.646	1.662
μ, mm^{-1}	2.072	5.182	4.863
F(000)	2960	548	1416
crystal size (mm^3)	0.43 × 0.37 × 0.16	0.25 × 0.20 × 0.10	0.30 × 0.15 × 0.10
2θ range (deg)	1.60 to 24.96	1.57 to 30.00	2.41 to 67.00
index ranges	$-15 \le h \le 15$	$-11 \le h \le 11$	$-14 \le h \le 14$
	$-22 \le k \le 22$	$-14 \le k \le 14$	$-15 \le k \le 15$
	$-29 \le l \le 29$	$-18 \le l \le 18$	$-22 \le l \le 22$
reflections collected	110435	41685	50256
independent reflections	10560	6522	9953
data/restraints/parameters	10560/168/896	6522/0/260	9953/18/811
goodness-of-fit on F^2	1.079	1.110	1.108
R1, wR2[$I > 2\sigma(I)$]	0.318, 0.0750	0.0274, 0.0765	0.0518, 0.1408
R1, wR2 (all data)	0.0374, 0.0778	0.0288, 0.073	0.00521, 0.1411

(10 mL) resulting in an olive green solution. Addition of 2,6-dimethylphenylisonitrile (6 mg, 0.046 mmol) at 0 °C caused a color change to red over 30 min of stirring. Addition of hexanes (25 mL) led to precipitation of a red solid (47 mg, 0.033 mmol, 79%). The product was dissolved in a small amount of diethyl ether and layered with hexanes in an inert atmosphere at −30 °C. After 3 days red-brown needles formed, and these were suitable for X-ray analysis. ^{1}H NMR (CD_2Cl_2, 298 K, δ): 7.26 (d, 2H, m-$C_6H_3Me_2$), 7.05 (t, 1H, p-$C_6H_3Me_2$), 5.82, 5.78 (each a s, each 1H, acac CH), 5.26 (s, 3H, N−CH_3), 4.61 (s, 3H, N=C−CH_3), 2.83, 2.51, 2.28, 2.13 (each a s, each 3H, acac CH_3), 2.51 (s, 6H, $C_6H_3(CH_3)_2$). ^{13}C{^{1}H} NMR (CD_2Cl_2, 298 K, δ): 18.7 ($C_6H_3(CH_3)_2$), 19.4

Table 3. Salient Crystallographic and Spectroscopic Data

complex	W−N (Å)	W−C (Å)	C−N (Å)	^{13}C, N≡*C* (δ)	^{13}C, *C*≡*C* (δ)	IR, ν_{CO} (cm^{-1})
CO-Nitrile[15]	2.018(5)	2.038(5)	1.270(7)	211.2	n/a	1895
1a[OTf][8]	1.977(7)	2.069(8)	1.283(10)	226.2	n/a	1976
CO-Imine[8]	1.905(5)	2.274(2)	1.383(2)	59.3, 60.6	n/a	1881, 1885
2c[BAr′$_4$]	1.963(9)	2.027(11)	1.323(14)	239.8	n/a	n/a
3b[BAr′$_4$]	1.957(3)	1.990(4)	1.324(5)	247.1	n/a	n/a
4[OTf]	n/a	n/a	n/a	50.9, 48.4	n/a	1904
5a[BAr′$_4$]	1.990(8)	2.052(9)	1.264(12)	217.0	204.6, 208.2	n/a
6	1.952(3)	2.220(3)	1.395(4)	76.2	204.7, 208.7	n/a
7[BAr′$_4$]	2.190(4)	2.168(5)	1.444(7)	91.4	240.1	n/a
8[BAr′$_4$]	1.925(3)	2.211(4)	1.395(5)	52.7	182.7, 182.8	n/a

(N=C−*C*H$_3$), 24.9, 25.1, 26.4, 27.9 (acac *C*H$_3$), 38.7 (N−*C*H$_3$), 98.7, 103.0 (acac *C*H), 128.1, 130.3, 137.2 (*C*$_6$H$_3$Me$_2$), 189.4, 190.0, 191.4, 200.0 (acac *C*O), 239.8 (N=*C*). HRMS (ESI) *m/z* Calc.: 569.164(M^+), 438.090 (M^+ − ArNC). Found: 569.166, 438.093.

[W(PPh$_3$)(η²-MeN=CPh)(acac)$_2$][OTf] (3a[OTf]). 1a[OTf] (61 mg, 0.090 mmol) was dissolved in methylene chloride (10 mL) in a 100 mL Schlenk flask resulting in a burgundy solution. Addition of triphenylphosphine (24 mg, 0.092 mmol) caused a color change to deep red-purple within 20 min. IR spectroscopy indicated no metal−carbonyl absorbances. Hexanes were added to precipitate a dark purple solid (79 mg, 0.087 mmol, 96%). ^{1}H NMR (CD_2Cl_2, 298 K, δ): 6.74 (s, 3H, N-C*H*$_3$), 6.02, 5.85 (each a s, each 1H, acac C*H*), 3.43, 2.84, 2.80, 2.07 (each a s, each 3H, acac C*H*$_3$). ^{13}C{^{1}H} NMR (CD_2Cl_2, 298 K, δ): 25.4, 26.2, 27.8, 34.9 (acac *C*H$_3$), 36.4 (N−*C*H$_3$), 98.9, 104.2 (acac *C*H), 189.0, 192.3, 196.5, 199.3 (acac *C*O), 241.1 (N=*C*). ^{31}P{^{1}H} NMR (CD_2Cl_2, 298 K, δ): −5.25 (s, *P*Ph$_3$, $^1J_{P-W}$ = 349 Hz).

[W(PCy$_3$)(η²-MeN=CPh)(acac)$_2$][OTf] (3b[OTf]). A 100 mL Schlenk flask was charged with **1a[OTf]** (56 mg, 0.083 mmol) and methylene chloride (15 mL) resulting in a burgundy solution. Addition of tricyclohexylphosphine (27 mg, 0.096 mmol) caused a color change to deep purple within 20 min. IR spectroscopy indicated no metal−carbonyl absorbances. Hexanes were added to precipitate at dark purple solid (75 mg, 0.081 mmol, 98%). ^{1}H NMR (CD_2Cl_2, 298 K, δ): 8.44 (br, s, 3H, N−C*H*$_3$), 7.98 (d, 2H, *o*-C$_6$*H*$_5$), 7.84 (t, 2H, *m*-C$_6$*H*$_5$), 7.23 (t, 1H, *p*-C$_6$*H*$_5$), 6.40, 5.97 (each a s, each 1H, acac C*H*), 4.11, 3.54, 2.83, 2.11 (each a s, each 3H, acac C*H*$_3$).^{13}C{^{1}H} NMR (CD_2Cl_2, 298 K, δ): 43.9 (br, N−*C*H$_3$), 98.2, 105.0 (acac *C*H), 127.6 (*m*-*C*$_6$H$_5$), 134.1 (*o*-*C*$_6$H$_5$), 136.8 (*p*-*C*$_6$H$_5$) 192.6, 199.3 (acac *C*O), 196.2, 202.3 (br, acac *C*O).^{13}C{^{1}H} NMR (CD_2Cl_2, 200 K, δ): 247.1 (N=*C*). ^{31}P{^{1}H} NMR (CD_2Cl_2, 298 K, δ): −23.2 (br, *P*Cy$_3$). ^{31}P{^{1}H} NMR ($CDCl_2F$, 160 K, δ): 18.0 (s, *P*Cy$_3$, $^1J_{P-W}$ = 351 Hz). MS (ESI) *m/z* Calc.: 780.3 (M^+), 500.1 (M^+ − PCy$_3$). Found: 780.4, 500.1.

[W(PCy$_3$)(η²-MeN=CPh)(acac)$_2$][BAr′$_4$] (3b[BAr′$_4$]). 3b[BAr′$_4$] was produced from **1a[BAr′$_4$]** in an analogous manner to **3b[OTf]**. The product was dissolved in a 50:50 mixture of diethyl ether and hexanes and placed in an inert atmosphere at −30 °C. Purple crystals suitable for X-ray diffraction formed in 2 weeks.

[W(PPh$_3$)(η²-MeN=CMe)(acac)$_2$][BAr′$_4$] (3c[BAr′$_4$]). A 100 mL Schlenk flask was charged with **1b[BAr′$_4$]** (50 mg, 0.038 mmol) and in methylene chloride (15 mL) resulting in an olive green solution. Addition of triphenylphosphine (20 mg, 0.076 mmol) caused a color change to red-purple within 2 h. The reaction was allowed to stir several hours under nitrogen to ensure completion. IR spectroscopy indicated no metal−carbonyl absorbances. Hexanes were added to precipitate a dark red-purple solid. The supernatant was removed via cannula, and the solid placed under vacuum (32 mg, 0.020 mmol, 54%). ^{1}H NMR (CD_2Cl_2, 298 K, δ): 7.34−7.50 (m, PPh$_3$), 5.80 (s, 3H, N−C*H*$_3$), 5.73, 5.40 (each a s, each 1H, acac C*H*), 4.06 (d, 3H, N=C−C*H*$_3$, $^4J_{P-H}$ = 1 Hz), 3.06, 2.23, 2.22, 2.11, (each a s, each 3H, acac C*H*$_3$). ^{13}C{^{1}H} NMR (CD_2Cl_2, 298 K, δ): 17.6 (N=C−*C*H$_3$), 23.9, 24.6, 26.5, 27.6 (acac *C*H$_3$), 36.8 (N−*C*H$_3$), 96.9, 102.4 (acac *C*H), 189.6, 191.1, 193.0, 200.8 (acac *C*O), 235.2 (d, N=*C*, $^2J_{P-C}$ = 36 Hz). ^{31}P{^{1}H} NMR (CD_2Cl_2, 298 K, δ): 7.46 (s, *P*Ph$_3$, $^1J_{P-W}$ = 305 Hz).

[W(CO)(η²-MeN-C(PMe$_3$)Ph)(acac)$_2$][OTf] (4[OTf]). 1a[OTf] (66 mg, 0.097 mmol) was dissolved in methylene chloride (15 mL) in a 100 mL Schlenk flask resulting in burgundy solution. Trimethylphosphine (20 μL, 0.19 mmol) was added causing a color change to red-brown. Reaction progress was monitored via in situ IR spectroscopy and was complete once a single CO absorbance appeared at 1904 cm^{-1}. Solvent volume was reduced in vacuo, and hexanes were added to precipitate a brown solid (62 mg, 0.081 mmol, 84%). IR (CH_2Cl_2): ν_{CO} = 1904 cm^{-1}; ^{1}H NMR (CD_2Cl_2, 298 K, δ, major diastereomer): 7.38−7.43 (m, 3H, *m* and *p*-C$_6$*H*$_5$), 7.08−7.10 (d, 2H, *o*-C$_6$*H*$_5$), 5.70, 5.64 (each a s, each 1H, acac C*H*), 4.07 (s, 3H, N−C*H*$_3$), 2.39, 2.22, 2.16, 2.12 (each a s, each 3H, acac C*H*$_3$), 1.97 (d, 9H, P−(C*H*$_3$)$_3$, $^2J_{P-H}$ = 13 Hz); ^{13}C{^{1}H} NMR (CD_2Cl_2, 298 K, δ, major diastereomer): 10.9 (d, P−(*C*H$_3$)$_3$, $^1J_{P-C}$ = 52 Hz), 25.3, 25.6, 27.8, 28.1 (acac *C*H$_3$), 43.7 (N−*C*H$_3$), 50.9 (d, N−*C*−P, $^1J_{P-C}$ = 84 Hz), 99.9, 102.7 (acac *C*H), 122.8 (*p*-*C*$_6$H$_5$), 127.1 (d, *o*-*C*$_6$H$_5$, $^3J_{P-C}$ = 3 Hz), 129.0 (*m*-*C*$_6$H$_5$), 142.0 (d, *ipso*-*C*$_6$H$_5$, $^2J_{P-C}$ = 30 Hz), 186.9, 187.2, 194.7, 196.2 (acac *C*O), 241.1 (d, *C*≡O, $^3J_{P-C}$ = 8 Hz); ^{31}P{^{1}H}NMR (CD_2Cl_2, 298 K, δ, major diastereomer): 49.1 (s, *P*Me$_3$).

W(η²-PhC≡CH)(η²-MeN=CPh)(acac)$_2$][BAr$_4$′] (5a[BAr′$_4$]). In the drybox, 125 mg of **1a[BAr′$_4$]** (0.090 mmol) was placed in a Schlenk tube. Methylene chloride was added (50 mL) followed by phenylacetylene (50 μL, 0.45 mmol). The vessel was placed in a photolysis chamber for 3 h, resulting in a color change from burgundy to light yellow. The solvent was removed in vacuo yielding a yellow/brown solid. Column chromatography on silica using methylene chloride eluted a dark yellow band (92 mg, 0.063 mmol, 70%). Yellow crystals suitable for X-ray diffraction formed in after few days via evaporation of a 50:50 mixture of methylene chloride and hexanes. IR (KBr): $\nu_{C\equiv C}$ = 1735 cm^{-1}. ^{1}H NMR (CD_2Cl_2, 298 K, δ, major isomer): 13.45 (s, 1H, PhC≡C*H*), 5.90, 5.88 (each a s, each 1H, acac C*H*), 3.80 (s, 3H, N−C*H*$_3$), 2.62, 2.60, 1.92, 1.86 (each a s, each 3H, acac C*H*$_3$). ^{1}H NMR (CD_2Cl_2, 298 K, minor isomer): 13.47 (s, 1H, PhC≡C*H*), 5.88, 5.63 (each a s, each 1H, acac C*H*), 4.21 (s, 3H, N−C*H*$_3$), 2.67, 2.48, 1.90, 1.80 (each a s, each 3H, acac C*H*$_3$). ^{13}C{^{1}H} NMR (CD_2Cl_2, 298 K, δ, major isomer): 25.2, 26.7, 28.3, 28.4 (acac *C*H$_3$), 38.7 (N−*C*H$_3$), 104.6, 105.1 (acac *C*H), 184.6, 189.0, 191.7, 195.1 (acac *C*O), 204.6 (PhC≡*C*H), 208.2 (Ph*C*≡CH), 217.0 (N=*C*). ^{13}C{^{1}H} NMR (CD_2Cl_2, 298 K, δ, minor isomer): 25.8, 26.4, 28.5, 28.9 (acac *C*H$_3$), 37.2 (N−*C*H$_3$), 104.3, 104.8 (acac *C*H), 186.5, 188.1, 192.2, 196.2

(acac *C*O), 206.4 (Ph*C*≡CH), 214.1 (PhC≡*C*H), 221.5 (N=*C*). Anal. Calcd for $WC_{58}H_{40}O_4F_{24}NB$: C, 47.54; H, 2.75; N, 0.96. Found: C, 47.52; H, 2.44; N, 1.06%.

[W(η^2-MeC≡CMe)(η^2-MeN=CPh)(acac)$_2$][BAr$_4$′] (5b[BAr′$_4$]). In the drybox, 270 mg of **1a[OTf]** (0.399 mmol) was placed in a Schlenk tube. Methylene chloride was added (60 mL) followed by 2-butyne (100 μL, 1.27 mmol). The tube was placed in a photolysis chamber for 3 h, resulting in a color change from burgundy to light yellow. Counterion exchange occurred by adding Na[BAr$_4$′] (350 mg, 0.0395 mmol) and stirring for 2 h. Column chromatography on silica using methylene chloride eluted a yellow band (367 mg, 0.259 mmol, 65%). ^{1}H NMR (CD_2Cl_2, 298 K, δ, major isomer): 5.83, 5.82 (each a s, each 1H, acac C*H*), 3.72 (s, 3H, N−CH_3), 3.19 (s, 6H, H_3C−C≡C−CH_3), 2.64, 2.55, 1.89, 1.81 (each a s, each 3H, acac CH_3). ^{1}H NMR (CD_2Cl_2, 298 K, δ, minor isomer): 5.86, 5.55 (each a s, each 1H, acac C*H*), 4.05 (s, 3H, N−CH_3), 3.17 (s, 6H, H_3C−C≡C−CH_3), 2.69, 2.46, 1.88, 1.75 (each a s, each 3H, acac CH_3). ^{13}C{^{1}H} NMR (CD_2Cl_2, 298 K, δ, major isomer): 18.4 (H_3C−C≡C−*C*H$_3$), 25.3, 26.8, 28.2, 28.5 (acac *C*H$_3$), 37.8 (N−*C*H$_3$), 104.1, 104.5 (acac *C*H), 185.2, 189.6, 191.6, 194.6 (acac *C*O), 211.0 (Me*C*≡*C*Me), 217.5 (N=*C*). Anal. Calcd for $WC_{54}H_{40}O_4NBF_{24}$: C, 45.75; H, 2.85; N, 0.99. Found: C, 45.96; H, 2.91; N, 0.89%.

[W(η^2-PhC≡CH)(η^2-MeN=CMe)(acac)$_2$][BAr$_4$′] (5c[BAr′$_4$]). In the drybox 50 mg of **1b[BAr′$_4$]** (0.038 mmol) was placed in a Schlenk tube. Methylene chloride was added (40 mL) followed by phenylacetylene (15 μL, 0.14 mmol). The vessel was placed in a photolysis chamber for 3 h, resulting in a color change from olive green to light yellow. The solvent was removed in vacuo yielding a yellow/brown solid. Column chromatography on silica using methylene chloride eluted a dark yellow band (38 mg, 0.027 mmol, 72%). ^{1}H NMR (CD_2Cl_2, 298 K, δ, major isomer): 13.25 (s, 1H, PhC≡C*H*), 5.84 (s, 2H, acac C*H*), 3.45 (s, 3H, N−CH_3), 3.15 (s, 3H, N=C−CH_3), 2.58, 2.55, 1.87, 1.86 (each a s, each 3H, acac CH_3). ^{1}H NMR (CD_2Cl_2, 298 K, minor isomer): 13.36 (s, 1H, PhC≡C*H*), 5.90, 5.73 (each a s, each 1H, acac C*H*), 3.76 (s, 3H, N−CH_3), 2.94 (s, 3H, N=C−CH_3), 2.61, 2.51, 1.87, 1.86 (each a s, each 3H, acac CH_3). ^{13}C{^{1}H} NMR (CD_2Cl_2, 298 K, δ, major isomer): 16.7 (N=C−*C*H$_3$), 25.0, 26.6, 28.3, 28.9 (acac *C*H$_3$), 37.6 (N−*C*H$_3$), 104.3, 105.1 (acac *C*H), 183.8, 188.8, 192.0, 195.6 (acac *C*O), 204.5 (PhC≡*C*H), 209.9 (Ph*C*≡CH), 229.0 (N=*C*). Anal. Calcd for $WC_{53}H_{38}O_4F_{24}NB$: C, 45.36; H, 2.73; N, 1.00. Found: C, 45.43; H, 2.67; N, 1.01%.

[W(η^2-MeC≡CMe)(η^2-MeN=CMe)(acac)$_2$][BAr$_4$′] (5d[BAr′$_4$]). In the drybox 50 mg of **1b[BAr′$_4$]** (0.038 mmol) was placed in a Schlenk tube. Methylene chloride was added (40 mL) followed by 2-butyne (0.10 mL, 1.28 mmol). The vessel was placed in a photolysis chamber for 3 h, resulting in a color change from olive green to light yellow. The solvent was removed in vacuo yielding a yellow/brown solid. Column chromatography on silica using methylene chloride eluted a dark yellow band (38 mg, 0.028 mmol, 75%). IR (KBr): $\nu_{C\equiv C}$ = 1764 cm^{-1}. ^{1}H NMR (CD_2Cl_2, 298 K, δ, major isomer): 5.79, 5.75 (each a s, each 1H, acac C*H*), 3.34 (s, 3H, N−CH_3), 3.12 (s, 6H, H_3C−C≡C−CH_3), 3.01 (s, 3H, N=C−CH_3), 2.56, 2.49, 1.84, 1.81 (each a s, each 3H, acac CH_3). ^{1}H NMR (CD_2Cl_2, 298 K, minor isomer): 5.82, 5.63 (each a s, each 1H, acac C*H*), 3.64 (s, 3H, N−CH_3), 3.08 (s, 6H, H_3C−C≡C−CH_3), 2.78 (s, 3H, N=C−CH_3), 2.63, 2.45, 1.84, 1.79 (each a s, each 3H, acac CH_3). ^{13}C{^{1}H} NMR (CD_2Cl_2, 298 K, δ): 15.7 (N=C−*C*H$_3$), 18.0 (H_3C−C≡C−*C*H$_3$), 25.1, 26.8, 28.4, 28.7 (acac *C*H$_3$), 36.7 (N−*C*H$_3$), 103.7, 104.3 (acac *C*H), 183.9, 189.2, 191.5, 195.2 (acac *C*O), 210.9 (Me*C*≡*C*Me), 230.1 (N=*C*). Anal. Calcd for $WC_{49}H_{38}O_4F_{24}NB$: C, 43.42; H, 2.83; N, 1.03. Found: C, 43.40; H, 2.73; N, 1.06%.

[W(η^2-MeC≡CMe)(η^2-MeNC(PMe$_3$)Ph)(acac)$_2$][BAr$_4$′] (6-[BAr′$_4$]). A Schlenk flask was charged with **5b[BAr′$_4$]** (52 mg, 0.037 mmol) and CH_2Cl_2 (15 mL) resulting in a yellow solution. Addition of PMe_3 (10 μL, 0.097 mmol) produced no visible color change over the course of stirring for 20 min. Hexanes (20 mL) were added to precipitate a pale yellow powder (32 mg, 0.021 mmol, 59%). Yellow crystals suitable for X-ray analysis were obtained by layering pentane over a methylene chloride solution of the product in an inert atmosphere and storing at −30 °C for several days. ^{1}H NMR (CD_2Cl_2, 298 K, δ, major diastereomer): 7.36 (br s, 3H, *o/m*-C$_6H_5$), 7.08 (t, 1H, *p*-C$_6H_5$), 6.30 (br s, 1H, *o*-C$_6H_5$), 5.75, 5.48 (each a s, each 1H, acac C*H*), 3.66 (s, 3H, N−CH_3), 2.78, 1.42 (each a s, each 6H, CH_3−C≡C−CH_3), 2.43, 2.34, 1.86, 1.76 (each a s, each 3H, acac CH_3), 1.71 (d, 9H, P−(CH_3)$_3$, $^2J_{P-H}$ = 13 Hz); ^{1}H NMR (CD_2Cl_2, 203 K, δ, major diastereomer): 7.27, 6.17 (each a d, each 1 H, *o*-C$_6H_5$, $^2J_{H-H}$ = 6 Hz), 7.38, 7.13 (each a t, each 1H, *m*-C$_6H_5$, $^2J_{H-H}$ = 6 Hz), 6.98 (t, 1H, *p*-C$_6H_5$, $^2J_{H-H}$ = 6 Hz), 2.69, 1.16 (each a s, each 6H, CH_3−C≡C−CH_3). ^{13}C{^{1}H} NMR (CD_2Cl_2, 203 K, δ, major diastereomer): 11.6 (d, P−(*C*H$_3$)$_3$, $^1J_{P-C}$ = 51 Hz), 13.0, 15.8 (*C*H$_3$−C≡C−*C*H$_3$), 25.9, 26.4, 27.4, 28.2 (acac *C*H$_3$), 42.9 (N−*C*H$_3$), 52.8 (N−*C*−PMe$_3$), 101.6, 102.7 (acac *C*H), 123.1, 125.4, 128.0, 141.7 (*C*$_6$H$_5$), 182.7, 182.8 (Me*C*≡*C*Me), 184.2, 185.5, 188.0, 191.6 (acac *C*O). ^{31}P NMR (CD_2Cl_2, 203 K, δ, major diastereomer): 35.1 (*P*Me$_3$). Anal. Calcd for $WC_{57}H_{49}BF_{24}NO_4P$: C, 45.84; H, 3.31; N, 0.94. Found: C, 45.82; H, 3.28; N, 0.83%.

[W(η^2-PhC=C(H)PMe$_3$)(η^2-MeN=CPh)(acac)$_2$][BAr$_4$′] (7-[BAr′$_4$]). A Schlenk flask was charged with **5a[BAr′$_4$]** (48 mg, 0.033 mmol) and CH_2Cl_2 (15 mL) resulting in a yellow solution. Addition of PMe_3 (10 μL, 0.097 mmol) produced no visible color change over the course of stirring for 20 min. Hexanes (20 mL) were added, and the solvent was removed to produce a yellow powder (35 mg, 0.023 mmol, 69%). ^{1}H NMR (CD_2Cl_2, 298 K, δ, major isomer): 5.81, 5.57 (each a s, each 1H, acac C*H*), 3.83 (s, 3H, N−CH_3), 3.04 (d, 1H, C=C−*H*, $^2J_{P-H}$ = 27 Hz), 2.25, 2.24, 1.94, 1.82 (each a s, each 3H, acac CH_3), 1.70 (d, 9H, P−(CH_3)$_3$, $^2J_{P-H}$ = 13 Hz); ^{13}C{^{1}H} NMR (CD_2Cl_2, 298 K, δ, major isomer): 13.0 (d, P−(*C*H$_3$)$_3$, $^1J_{P-C}$ = 55 Hz), 26.3, 27.5, 27.7, 28.1 (acac *C*H$_3$), 31.6, (d, C=*C*(H)PMe$_3$, $^1J_{P-C}$ = 85 Hz), 35.3 (N−*C*H$_3$), 102.2, 102.4 (acac *C*H), 185.4, 187.0, 190.5, 190.9 (acac *C*O), 218.2 (N=*C*), 240.9 (*C*=C(H)PMe$_3$); ^{31}P NMR (CD_2Cl_2, 298 K, δ, major isomer): 34.8 (*P*Me$_3$, $^2J_{P-W}$ = 34 Hz).

W(η^2-MeC≡CMe)(η^2-MeN=CHPh)(acac)$_2$ (8). 5b[OTf] was generated in situ from **1a[OTf]** (210 mg, 0.310 mmol) according to the above procedure. The solvent was removed, and the solid was washed with hexanes (40 mL). The brown powder was dissolved in THF (10 mL) resulting in a brown solution. In a separate flask, Na[HB(OMe)$_3$] (50 mg, 0.39 mmol) was dissolved in THF (7 mL). This solution was cannula transferred to the flask containing **5b[OTf]** resulting in a color change from brown to dark orange. The solvent volume was reduced in vacuo after 15 min of stirring, and hexanes (40 mL) were added to precipitate residual salts. The supernatant was cannula filtered to a separate flask, and the remaining solvent was removed in vacuo yielding an orange solid. Purification occurred via column chromatography on silica using a mixture of CH_2Cl_2 and diethyl ether (90:10) to elute an orange band (119 mg, 0.214 mmol, 69%). Orange crystals suitable for X-ray analysis formed after a few days in a concentrated pentane solution at −30 °C. ^{1}H NMR (CD_2Cl_2, 200 K, δ, major isomer): 5.50, 4.69 (each a s, each 1H, acac C*H*), 3.43 (s, 3H, N−CH_3),

3.08, 2.62 (each a s, each 3s, $H_3C-C\equiv C-CH_3$), 2.45, 1.90, 1.68, 1.59 (each a s, each 3H, acac CH_3), 2.40 (s, 1H, $N=C-H$). $^{13}C\{^1H\}$ NMR (CD_2Cl_2, 200 K, δ, major isomer): 15.3, 17.9 ($H_3C-C\equiv C-CH_3$), 26.2, 26.3, 27.9, 28.4 (acac CH_3), 45.8 ($N-CH_3$), 73.6 ($N=C$), 98.8, 101.3 (acac *C*H), 147.0 (*ipso*-C_6H_5), 184.7, 186.5, 188.1, 191.0 (acac *C*O), 204.7, 208.7 (Me*C*≡*C*Me). Anal. Calcd for $WC_{22}H_{29}O_4N$: C, 47.58; H, 5.27; N, 2.52. Found: C, 47.74; H, 5.10; N, 2.50%.

[W(η^2-MeC≡CMe)(η^2-$Me_2N=CHPh$)(acac)$_2$][BAr$_4'$] (9[BAr$'_4$]). In a Schlenk flask **8** (338 mg, 0.609 mmol) was combined with methylene chloride (15 mL) resulting in an orange solution. Methyl trifluoromethylsulfonate (MeOTf) was added (50 μL, 0.44 mmol), and the reaction mixture was allowed to stir for 2 h. The solvent volume was reduced in vacuo, and hexanes (40 mL) were added to aid in precipitating an orange solid. The supernatant was removed via cannula filtration. For counterion exchange, the product was dissolved in methylene chloride (15 mL) and combined with Na[BAr′$_4$] (540 mg, 0.609 mmol). The reaction mixture was allowed to stir for 4 h, at which point the orange liquid was cannula filtered away from residual salt to a separate flask and the solvent was removed in vacuo. Purification of the orange solid was achieved via column chromatography on silica using methylene chloride to elute an orange band (542 mg, 0.378 mmol, 62%). Orange needles suitable for X-ray analysis were obtained via evaporation of a solution of 50:50 methylene chloride and hexanes. ^1H NMR (CD_2Cl_2, 298 K, δ, major isomer): 7.45 (t, 2H, *m*-C_6H_5), 7.32 (d, 2H, *o*-C_6H_5), 7.17 (s, 1H, *p*-C_6H_5), 5.98, 5.73 (each a s, each 1H, acac C*H*), 3.99 (s, 1H, $N=C-H$), 2.97, 2.64 (each a s, each 3H, $N-CH_3$), 2.82 (s, 6H, $CH_3-C\equiv C-CH_3$), 2.50, 2.49, 2.01, 1.83 (each a s, each 3H, acac CH_3). $^{13}C\{^1H\}$ NMR (CD_2Cl_2, 298 K, δ, major isomer): 19.8 ($CH_3-C\equiv C-CH_3$), 25.1, 26.8, 28.4, 28.6 (acac CH_3), 51.4, 53.1 ($N-CH_3$), 91.4 ($N=C$), 103.7, 105.5 (acac *C*H), 184.2, 188.8, 194.5, 194.9 (acac *C*O), 240.1 (Me*C*≡*C*Me). Anal. Calcd for $WC_{55}H_{44}O_4NBF_{24}$: C, 46.08; H, 3.10; N, 0.98. Found: C, 46.32; H, 3.39; N, 0.83%.

Acknowledgment. We thank the National Science Foundation (CHE-0717086) for financial support, and Dr. Matthew C. Crowe and Dr. Sohrab Habibi for mass spectral measurements.

Supporting Information Available: Full details of the crystal structure analyses for **2c[BAr′$_4$]**, **3b[BAr′$_4$]**, **4[BAr′$_4$]**, **5a[BAr′$_4$]**, **6[BAr′$_4$]**, **8,** and **9[BAr′$_4$]** in CIF format and NMR spectra of **3a[OTf]**, **3b[OTf]**, **4[OTf]**, **6[BAr′$_4$]**, and **7[BAr′$_4$]**. This material is available free of charge via the Internet at http://pubs.acs.org.

IC800738A